Preprint
UCRL-JC-145171

1 – 10 Mbar Laser-Driven Shocks Using the JANUS Laser

J. Dunn, D.F. Price, S.J. Moon, R.C. Cauble, P.T. Springer, A. Ng

This article was submitted to:
12th Biennial International Conference of the APS Topical Group on "Shock Compression of Condensed Matter", Atlanta, Georgia, 24-29 June, 2001.

U.S. Department of Energy

Lawrence Livermore National Laboratory

August, 10 2001

1 – 10 MBAR LASER-DRIVEN SHOCKS USING THE JANUS LASER FACILITY

James Dunn[1], Dwight F. Price[1], Stephen J. Moon[1], Robert C. Cauble[1], Paul T. Springer[1], and Andrew Ng[2]

[1] *University of California, Lawrence Livermore National Laboratory, Livermore, CA 94551*
[2] *Dept. Of Physics and Astronomy, University of British Columbia, Vancouver, Canada*

Abstract. We report preliminary results using the Lawrence Livermore National Laboratory (LLNL) Janus laser facility to generate high pressure laser-driven shocks in the 1 – 10 Mbar regime. These experiments address various issues, including shock steadiness, planarity, uniformity and low target pre-heat, important for making precision EOS measurements on a small (E < 250 J) laser facility. A brief description of the experimental techniques, target design and measurements will be given.

INTRODUCTION

The use of high-power laser pulses focused to high intensities is a well-established technique and one way to shock compress materials at the Mbar (100 GPa) level [1–3]. Many direct-drive laser experiments have been performed to characterize the principal Hugoniots of Al [4], Cu [5] and liquid D_2 [6] to compare with equation-of-state (EOS). Indirect-drive experiments using laser beams focused in hohlraum cavities have also been conducted to improve the shock uniformity [5, 7, 8].

Laboratory gas gun experiments have been conducted to benchmark Hugoniot measurements for various materials including Al, Cu, and Ta undergoing shock compression in the 0 – 5 Mbar regime [9]. The gas gun type experiments have a number of important properties that allow precise determination of the shock pressure and EOS properties: (1) the initial conditions before the shock arrives are well characterized; (2) the launched shocks are planar, uniform, and steady; (3) the particle and shock velocities are accurately measured, the former determined by radiography of the impactor in flight. The number of gas gun shots, in common with large laser facilities, tends to be limited as a result of cost and setup time. Further review of gas gun experiments and additional references can be found in ref. [10].

Smaller laser facilities have the advantage of allowing a larger number of shots on target than the larger national facilities e.g. OMEGA and previously on NOVA. These laser shots are at lower shock pressures but more time can be dedicated to studying important details of the experiment, in particular, shock steadiness, planarity, uniformity and low target pre-heat. In this work, we address some of these issues for laser-driven shocks using the LLNL Janus laser facility in an initial set of experiments.

EXPERIMENTAL DESCRIPTION

The shock experiments were conducted on the LLNL Janus laser. This is a two-beam facility with pulse durations available from 100 ps to 7 ns (FWHM). For this work, a single beam of a 5 ns square pulse shape with a ~200 ps risetime was generated by utilizing a fast Pockels Cell switchout from a 7 ns (FWHM) Gaussian laser pulse. The 5 ns square pulse was determined from LASNEX hydrodynamic code simulations to give the desired combination of steady shocks and optimum pressures for the experiment. Output energy up to 220 J, 1064 nm wavelength, was available with 82.5% delivered on target. Laser energy losses were mainly associated with the uncoated debris shield and the Phase Zone Plate (PZP) optic. The laser repetition rate was 1 shot/30 minutes with 8 shots/day being regularly achieved. This shot rate together with the total number of shots available is substantially higher than larger laser facilities and gas gun experiments.

The shock pressure is determined by the maximum intensity of the focused laser beam hence high pressures of 1 – 10 Mbars or higher require intensities of 10^{13} – 10^{14} W cm^{-2}. A large focal spot, width w, is essential to launch a planar shock without shock erosion at the edges through a target of thickness z. Generally, $w > 5z$ is desired for good planarity in the center part of the laser focus driving the shock. For this experiment with target thickness z of ~ 100 µm the highest pressure possible was less important than having large, smooth, planar shocks. A ~500µm (FWHM) smoothed focal spot with a Super Gaussian (n=3.4) profile was achieved by using a PZP optic in combination with an f=34.3 cm focal length, f#3 aspherical lens [11], shown in Fig. 1. The PZP optic contains an array of Fresnel lenses which by sampling the laser spatial beam profile at different positions maps any low frequency beam non-uniformities into a uniform high-frequency speckle pattern at the focus [12, 13]. Plasma ablation and shock propagation through the initial few microns of target smoothes the high frequency micron scale speckle leaving a planar uniform shock.

LASNEX simulations were performed to design a target to minimize target pre-heat at the sample before the arrival of the shock. This is shown in Fig. 2. The generic target design consists of a 10 µm C_8H_8 (parylene-N, ρ=1.11g/cm^3) ablator layer coated onto a 25 µm Al (1100 alloy or high purity) pusher layer and finally the sample to be studied. The low Z CH ablator gives good absorption of the laser energy into launching a shock but also minimizes the coupling of the laser energy into keV x-rays which together with hot electrons from the laser-produced plasma can be a source of sample pre-heat. The simulations indicated that a 25 µm thick Al pusher was sufficient to filter the keV x-rays and keep pre-heat at the pusher/sample interface to a minimum.

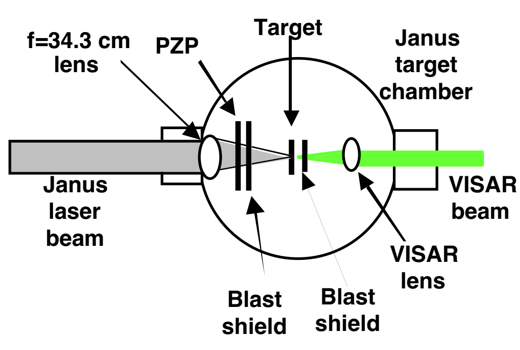

FIGURE 1. Setup showing Janus drive and VISAR probe.

The main shock diagnostic was a Velocity Interferometer for Any Reflector (VISAR) probe beam that monitored the back surface of the target [14, 15]. The velocity of the interface between the sample or the free surface can be measured and thus the particle velocity determined. A caveat is that the surface has to remain reflective during the motion. A powerful application of velocity interferometry is the ability to measure shock propagation inside a transparent medium if the shock pressure is high enough to metallize the material [6, 15]. The VISAR instrumentation used here was similar to that of Celliers *et al* [15]. A 14 ns (FWHM), 532 nm wavelength beam from a

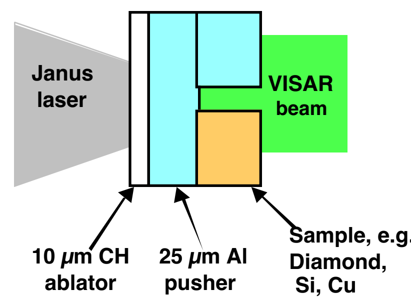

FIGURE 2. Target design showing CH ablator, Al pusher and sample to be shocked.

frequency-doubled Q-switched Nd:yttrium-aluminum-garnet (YAG) laser was synchronized to the main Janus laser drive to probe the target back surface during and after the launch of the shock wave. A variety of etalon lengths were used from 0.125 – 8 cm giving a velocity sensitivity of 38 – 0.6 µm/ns/fringe, respectively. The back surface was imaged with 10× magnification using an f=15 cm achromat and imaged onto the entrance slit of an S-20 photo-cathode Kentech or Hamamatsu streak camera. A time-resolved 1-dimensional line image of the shock breakout at the back of the target was obtained.

A custom target wheel consisting of a 5 cm diameter disk with 12 target positions was designed. Each target sat in a 1 cm diameter disk with a 0.3 cm aperture on center to allow the laser drive beam onto the ablator side of the target. Eleven targets were mounted radially on the target wheel in machined recesses with a cross-wire alignment fiducial on the 12^{th} position. The target alignment and positioning could be performed offline. After each laser shot, an encoded stepper-motor rotation stage allowed the next target to be aligned giving a fast time between shots. An anti-reflection (AR) coated fused silica blast shield placed behind the target prevented target debris from coating the VISAR imaging lens.

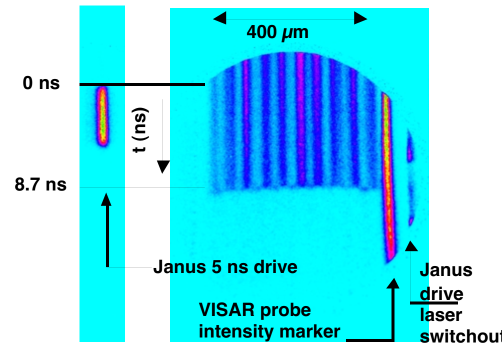

FIGURE 3. Streaked image showing planar shock breakout of 10 μm CH/100 μm Al foil at t = 8.7 ns.

RESULTS AND DISCUSSION

A simple target using 10 μm CH ablator vapor-deposited on various Al pusher foil thicknesses of 25 – 100 μm was constructed to determine shock planarity. The critical element in achieving smooth, planar shocks was the focusing of the main optic (*f*#3 asphere) and the Phase Zone Plate combination on the front of the target. The VISAR imaging achromat was used to focus the probe beam on the back surface of the target using a CCD imaging system built into the VISAR design. Then the same optic was used to focus the main Janus drive laser. Optimum (smooth) beam quality is achieved away from best focus [12]. Two sets of experiments were performed where the drive laser was focused in either the converging or diverging beam. The second diverging beam experiments gave more consistent, repeatable results for planar shocks.

A planar shock launched through a thin ~25 μm Al foil was fairly straightforward as a result of the fast shock transit time (~2 ns) and large *w*/*z* ratio (~14). A thicker Al foil is more demanding to maintain shock planarity as a result of progressive erosion at the edges of the shock as it propagates through the material. Figure 3 shows the shock breakout for a 10 μm CH/100 μm Al foil driven at a laser intensity of 1.2×10^{13} W cm^{-2} generating a shock pressure in the 1 – 1.5 Mbar range. At the left side, the start of the Janus 5 ns square laser drive is indicated at 0 ns and the shock breakout of the Al foil is 8.7 ns later. At shock breakout the VISAR signal disappears simultaneously in a uniform and planar manner across about 400 μm of the foil. The VISAR probe is still incident on the foil, as indicated by the intensity marker on the right. The loss of the VISAR signal may be due to a drop in the Al reflectivity from shock melting or absorption in a dense vapor layer close to the foil surface. Melting on the shock Hugoniot is predicted to begin at 1.2 Mbars and end at about 1.55 Mbars [16].

Al foil targets of different thickness, with and without CH ablator, were irradiated at 1.2×10^{13} W cm^{-2} to determine the effectiveness of a low *Z* ablator for reducing pre-heat. A 5.5 cm etalon was used in the VISAR to give a velocity sensitivity of 0.92 μm/ns/fringe. Motion of the back surface of the foil before shock breakout would indicate target pre-heat. Figure 4(a) shows that with the 10 μm CH ablator on a 25 μm foil no pre-heat could be detected before shock breakout at 4.05 ns. The laser pulse starts at 2 ns. This gives an upper limit on the pre-heat of $\Delta T \sim 0.01$ eV. Figure 4(b) for a thinner 12.5 μm Al foil with no CH ablator clearly shows fringe motion starting 0.48 ns before breakout and reaching a maximum velocity of 0.73 μm/ns at 3.0 ns. Estimates of the pre-heat

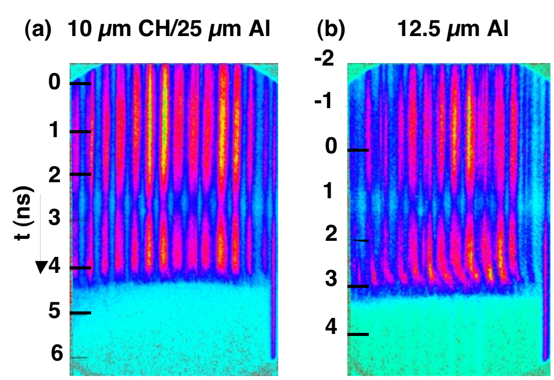

FIGURE 4. (a) Streaked image of 10 μm CH /25 μm Al shows no back surface motion before breakout at 4.05 ns. (b) 12.5 μm Al with no ablator showing back surface movement before breakout at 3.0 ns. In each case the laser pulse starts at 2 ns. Note that the change in the fringe reflectivity at 2.5 ns on Fig. 4(a) and at 1.0 ns on Fig. 4(b) is due to an artifact of the streak camera.

level are 0.05 – 0.1 eV. Further analysis and modeling of these results are under way but the effect of the ablator in reducing pre-heat is demonstrated.

Shock velocity and steadiness were determined by measuring the time of shock breakout from a stepped Al target of maximum step thickness 125 μm with a 10 μm CH ablator. Figure 5 shows that for 10^{13} W cm^{-2}, u_s = 10.65 μm/ns and the velocity was constant to within 2.5%. This corresponds to a shock pressure of 1.12 Mbar (based on the u_s vs u_p relations from ref. [9]). A maximum pressure of 1.6 Mbar was achieved in Al in this experiment though higher pressure ~4 Mbar was achieved when higher density samples e.g. diamond were placed behind the Al pusher layer.

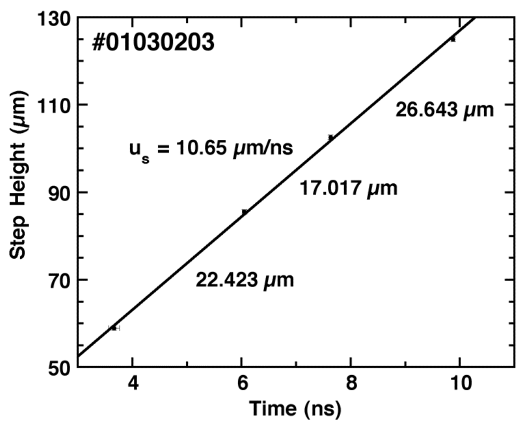

FIGURE 5. Shock breakout for Al step height versus breakout time.

CONCLUSIONS

We have conducted a few Megabar pressure experiments on the LLNL Janus facility at intensities ~1 – 2 × 10^{13} W cm^{-2}. The target design has been optimized under these conditions to give steady, planar shocks with very low pre-heat. More detailed analysis and comparisons with simulations will be reported at a later date.

ACKNOWLEDGMENTS

The authors would like to thank Jim Emig, Derek Decker, and Al Ellis for their technical contributions to instrumentation and target fabrication in this research. This work was performed under the auspices of the US Department of Energy by the University of California Lawrence Livermore National Laboratory under Contract No. W-7405-Eng-48.

REFERENCES

1. Veeser, L., and Solem, J., *Phys. Rev. Lett.* **40**, 1391 – 1394 (1978).
2. Trainor, R. J., Shaner, J. W., Auerbach, J. M., and Holmes, N. C., *Phys. Rev. Lett.* **42**, 1154 – 1157 (1979).
3. Cottet, F., Romain, J. P., Fabbro, R., and Faral, B., *Phys. Rev. Lett.* **52**, 1884 – 1887 (1984).
4. Ng, A., Parfeniuk, D., and Da Silva, L., *Phys. Rev. Lett.* **54**, 2604 – 2607 (1985).
5. Benuzzi, A., Löwer, T., Koenig, M., Faral, B., Batani, D., Beretta, D., Danson, C., and Pepler, D., *Phys. Rev. E.* **54**, 2162 – 2165 (1996).
6. Da Silva, L. B., Celliers, P., Collins, G. W., Budil, K. S., Holmes, N. C., Barbee Jr., T.W., Hammel, B. A., Kilkenny, J. D., Wallace, R. J., Ross, M., Cauble, R., Ng, A., and Chiu, G., *Phys. Rev. Lett.* **78**, 484 – 487 (1997).
7. Löwer, T., Sigel, R., Eidmann, K. , Földes, I. B., Hüller, S., Massen, J., Tsakiris, G. D., Witkowski, S., Preuss, W., Nishimura, H., Shigara, H., Kato, Y., Nakai, S., and Endo, T., *Phys. Rev. Lett.* **72**, 3186 – 3189 (1994).
8. Evans, A. M., Freeman, N. J., Graham, P., Horsfield, C. J., Rothman, S. D., Thomas, B. R., and Tyrrell, A.J., *Laser and Particle Beams*, **14**, 113 – 123 (1996).
9. Mitchell, A. C., and Nellis, W. J., *J. Appl. Phys.* **52**, 3363 – 3374 (1981).
10. Nellis, W. J., *Encyclopedia. Appl. Phys.* **18**, 541 – 554 (1997).
11. Dunn, J., unpublished data (2001).
12. Stevenson, R. M., Norman, M. J., Bett, T. H., Pepler, D. A., Danson, C. N., Ross, I. N., *Opt. Lett.* **19**, 363 (1994).
13. Koenig, M., Faral, B., Boudenne, J.-M., Batani, D., Benuzzi, A., and Bossi, S., *Phys. Rev. E.* **50**, R3314 – 3317 (1994).
14. Barker, L.M., and Hollenbach, R.E., *J. Appl. Phys.* **43**, 4669 (1972).
15. Celliers, P. M., Collins, G. W., Da Silva, L. B., Gold, D. M., and Cauble, R., *Appl. Phys. Lett.* **73**, 1320 – 1322 (1998).
16. Moriarty, J. A., Young, D.A., and Ross, M., *Phys. Rev. B* **30**, 578 – 588 (1984).

University of California
Lawrence Livermore National Laboratory
Technical Information Department
Livermore, CA 94551